Available online at www.sciencedirect.com

ScienceDirect

journal homepage: www.jfda-online.com

Original Article

Proteomic changes associated with metabolic syndrome in a fructose-fed rat model

Cheng-Chu Hsieh [a,b,1], Chen-Chung Liao [c,1], Yi-Chun Liao [d,1], Lucy Sun Hwang [e], Liang-Yi Wu [f], Shu-Chen Hsieh [e,*]

[a] Department and Institute of Veterinary Medicine, School of Veterinary Medicine, National Taiwan University, Taipei, Taiwan
[b] Biologics Division, Animal Health Research Institute, Council of Agriculture, Executive Yuan, New Taipei, Taiwan
[c] Proteomics Research Center, National Yang-Ming University, Taipei, Taiwan
[d] Department of Biochemical Science and Technology, National Taiwan University, Taipei, Taiwan
[e] Institute of Food Science and Technology, National Taiwan University, Taipei, Taiwan
[f] Department of Bioscience Technology, Chung Yuan Christian University, Taoyuan City, Taiwan

ARTICLE INFO

Article history:
Received 16 February 2016
Received in revised form
16 March 2016
Accepted 23 March 2016
Available online 24 June 2016

Keywords:
endoplasmic reticulum stress
fructose
insulin resistance
metabolic syndrome
oxidative stress

ABSTRACT

Metabolic syndrome (MetS), characterized by a constellation of disorders such as hyperglycemia, insulin resistance, and hypertension, is becoming a major global public health problem. Fructose consumption has increased dramatically over the past several decades and with it the incidence of MetS. However, its molecular mechanisms remain to be explored. In this study, we used male Sprague-Dawley (SD) rats to study the pathological mechanism of fructose induced MetS. The SD rats were fed a 60% high-fructose diet for 16 weeks to induce MetS. The induction of MetS was confirmed by blood biochemistry examination. Proteomics were used to investigate the differential hepatic protein expression patterns between the normal group and the MetS group. Proteomic results revealed that fructose-induced MetS induced changes in glucose and fatty acid metabolic pathways. In addition, oxidative stress and endoplasmic reticulum stress-related proteins were modulated by high-fructose feeding. In summary, our results identify many new targets for future investigation. Further characterization of these proteins and their involvement in the link between insulin resistance and metabolic dyslipidemia may bring new insights into MetS.

* *Corresponding author*. Institute of Food Science and Technology, College of Bioresources and Agriculture, National Taiwan University, Number 1, Section 4, Roosevelt Road, Taipei 10617, Taiwan.
E-mail address: schsieh@ntu.edu.tw (S.-C. Hsieh).
[1] These authors contributed equally to this study.

http://dx.doi.org/10.1016/j.jfda.2016.03.005

1. Introduction

Metabolic syndrome (MetS), which involves obesity, insulin resistance, hypertension, and hyperlipidemia, is becoming a major global public health problem [1,2]. The modern lifestyle of an increased intake of a palatable high-fat diet in association with decreased energy expenditure contributes to the current rising prevalence of MetS [2,3]. Metabolic syndrome is complex and encompasses several interrelated disturbances of glucose and lipid homeostasis [4,5]. The major risk factors for MetS are abdominal obesity, elevated fasting plasma glucose, atherogenic dyslipidemia (i.e., increased levels of triacylglyerols, increased levels of low-density lipoprotein, and decreased levels of high-density lipoprotein), the presence of prothrombotic and proinflammatory states, and elevated blood pressure [6]. The most important interacting features of MetS have been proposed by Grundy [6] as obesity plus endogenous metabolic susceptibility, which is manifested by insulin resistance and other factors such as genetic factors, physical inactivity, advancing age, and endocrine dysfunction.

Fructose, which occurs naturally in honey and sweet fruits, is produced in crystalline and syrup forms for commercial use. The most commonly used form, corn syrup, contains approximately 55% free fructose. Its use as a sweetener in processed foods and soft drinks has increased by 20–30% over the past 20 years in the United States, similar to the dramatic rise in obesity over the same period [7]. The metabolic effects of fructose and its use by individuals with metabolic disorders have attracted much attention over the past two decades. Fructose has unique metabolic features because it is largely metabolized by splanchnic organs (i.e., gut and liver cells) through insulin-independent mechanisms. Fructose is involved in the progression to MetS through the dysregulation of many molecular signaling factors [7,8]. Animal model experiments have clearly demonstrated that fructose feeding in rats causes hypertension and hyperinsulinemia [9], and in hamsters causes insulin resistance, hypertriglyceridemia, hepatic very-low-density lipoprotein overproduction, obesity, and hyperglycemia [10,11].

Proteomics involves integrating several technologies with the aim of systematically analyzing the complement of proteins expressed in a biological system in response to specific stimuli and different physiological or pathological conditions. Examining changes in the proteome offers insights into cellular and molecular mechanisms that cannot always be obtained through genomic analysis. The information gap between the genome and cellular processes can be largely attributed to post-translational modifications such as phosphorylation and glycosylation. These modifications, which cannot be monitored by genomic analyses alone, modulate important regulatory processes such as protein turnover, protein activity, and protein localization within a cell.

In the current study, we employed the electrospray ionization-tandem mass spectrometry (ESI-MS/MS) proteomics approach to identify candidate molecules that link high-fructose consumption to the pathogenesis of MetS. Our results showed that high-fructose feeding was associated with significant alterations in the expression of hepatic enzymes in multiple pathways. In addition to the marked upregulation of hepatic functions that promote triglyceride synthesis and very-low-density lipoprotein-triglycerides production, high-fructose consumption also resulted in perturbations of antioxidant functions in protein folding.

2. Methods

2.1. Establishment of the high-fructose diet-induced MetS rat model

Male Sprague–Dawley (SD) rats weighing 200–250 g were housed two animals per cage in an air-conditioned room (22°C ± 2°C) on a 12 hour light cycle (7:00 AM to 7:00 PM). The animals were maintained in accordance with the guidelines established in the Taiwan Government Guide for the Care and Use of Laboratory Animals. In this study, we used a well-established rat model in which insulin resistance, hypertension, and dyslipidemia can be induced by feeding the animals a high-fructose diet [12,13]. Rats were randomly divided into two groups: Group I, which was fed the standard Purina chow (#5001, Purina, St. Louis, MO, USA; consisting of 23% protein, 56% carbohydrate, 4.5% fat, and 6% fiber), and Group II, which was fed a 60% high-fructose diet plus the supplement of 21% protein, 5% fat, and 8% fiber. The dietary manipulation lasted for 16 weeks. Blood pressure was measured every week, total cholesterol concentrations were measured every 2 weeks, and an oral glucose tolerance test was performed every 4 weeks. At the end of the experiment, blood pressure was measured, and the rats were decapitated after overnight fasting. Blood samples were collected in heparinized tubes, and the plasma was separated by centrifugation and stored at −20°C until assayed for glucose, insulin, triglyceride, cholesterol, and thiobarbituric acid-reactive substances. The livers were stored in liquid nitrogen and subjected to two-dimensional (2-D) gel-based proteomics.

2.2. Tissue harvest

Frozen livers were crushed in liquid nitrogen into a fine powder. The resulting powder was dissolved in a lysis buffer [7M urea, 2 M thiourea, 4% w/v 3-[(3-cholamidopropyl)dimethylammonio]-1-propanesulfonate (CHAPS), 0.5% Triton X-100, and 10 mM dithiothreitol (DTT)] containing a cocktail of protease inhibitors (cOmplete™ Mini, Roche, Mannheim, Germany) and centrifuged at 4°C and 16,000 × *g* for 60 minutes. The supernatant was used as the tissue protein lysate.

2.3. Two-dimensional gel electrophoresis and protein labeling

The protein concentration was determined using the PlusOne 2-D Quant Kit (Amersham Biosciences, Piscataway, NJ, USA) in accordance with the manufacturer's manual. Approximately 150 μg of protein was dissolved in 350 μL of rehydration buffer (7M urea, 2 M thiourea, 1% w/v CHAPS, 0.5% Triton X-100, 100 mM DTT and 0.2% v/v immobilized pH gradient buffer, pH 3–11, nonlinear; Amersham Biosciences) and applied to an 18 cm, nonlinear pH 3–10 Immobiline DryStrip (Amersham

Biosciences) for in-gel rehydration. Fifty micrograms of liver protein from the control group and MetS induced group were labeled with Cy3 and Cy5 dyes, respectively. The reaction was then quenched with 10mM lysine for 10 minutes. The labeled Cy3- and Cy5-treated samples were combined with 8 μL of DeStreak (GE Healthcare, Little Chalfont, Buckinghamshire, UK) and 4 μL of pH 3-10 ampholytes (GE Healthcare). The solution volume was adjusted to 440 μL with the necessary volume of rehydration solution. One-dimension isoelectric focusing (IEF) was performed on a Protean IEF system (BioRad, Hercules, CA, USA) using the following program: 0 V × 12 hours; 50 V × 1 hour; 300 V × 1 hour; 600 V × 1 hour; 1500 V × 2 hours; and 2500 V × 2 hours. The gradient was raised from 2500 V to 8000 V within 2 hours, and IEF was terminated after a total of 54,000 V/hour. Before separating on sodium dodecyl sulfate polyacrylamide gel electrophoresis (SDS-PAGE), the focused immobilized pH gradient strips were equilibrated in an equilibrium buffer (50 mM Tris-Cl, pH 8.8, 6 M urea, 30% v/v glycerol and 2% w/v SDS) containing 1% w/v DTT for 15 minutes, and then soaked in the same buffer containing 2.5% w/v iodoacetamide for 15 minutes. The strips were then placed on a 10% acrylamide: *bis*-acrylamide (37:1) SDS-PAGE gel and immobilized with agarose sealing solution (0.5% w/v agarose, 25 mM Tris, 192 mM glycine, 0.1% w/v SDS, and a trace of bromophenol blue). The second-dimensional SDS-PAGE was performed at 25 mA per gel until the bromophenol blue dye front reached the bottom of the gel. The Cy3 gels were scanned at 580 Bp30 with a green laser (532 nm), and Cy5 gels were scanned at 670 Bp30 with a red laser (633 nm). Gels utilized for mass spectroscopy (MS) analysis were run with 500 μg of protein. Plates were separated, and the gels were fixed overnight in 30% methanol/10% glacial acetic acid and stained overnight in Sypro Ruby dye (Molecular Probes™, Thermo Fisher Scientific, Waltham, MA, USA). Differential gel presentation was created within a custom-written image processing program (i.e., Interactive Data Language, Remote Sensing Image) to correct for scanning detector alterations for the different wavelengths. Large differences in protein contents were observed in some of these studies; therefore, global corrections were inadequate. For this procedure, a nonscaled color overlay of the Cy3 and Cy5 images was used to select a region of interest (ROI) for use in the scaling function. The ROI was selected based on the area of the gel in which there was high signal-to-noise difference in Cy3 and Cy5 with minimal background noise; this optimized the linear least-squares approach using the scaling function. In general, the ROI represented <20% of the total image.

2.4. *Mass spectrometry*

Gel spots of interest were destained three times with 100 μL 25 mM ammonium bicarbonate (NH_4HCO_3)/50% v/v acetonitrile (ACN) for 15 minutes. The solution was then removed and 100 μL of 100% ACN was added to dehydrate the gel pieces. Thereafter, 1.6 μL of 20 ng/μL trypsin (Promega, Fitchburg, WI, USA) in 25 mM NH_4HCO_3 was added to the gel pellets and they were maintained at 4°C for 40 minutes. An extra 2 μL of 25 mM NH_4HCO_3 was added, and the reaction was incubated overnight at 37°C. Finally, 5 μL of 1% trifluoroacetic acid in 50% aqueous ACN was added and gel pieces were sonicated with 7 μL 1% formic acid for 15 minutes to release the tryptic peptides for the following MS-based protein identification. The MS/MS analyses were performed using a Q-TOF-2 system (Waters, Milford, MA, USA) to identify the selected proteins. The tryptic peptides were separated on a reversed-phase capillary C18 column (20 μm id × 90 μm id) and directed to the electrospray source of the mass spectrometer. The mass spectrometer was operated in positive ion mode with a source temperature of 80°C and a cone voltage of 45 V. A voltage of 3.2 kV was applied to the source capillary. The time-of-flight analyzer was set in the V-mode. The MS/MS spectra were obtained in the data-dependent acquisition mode whereby the two multiple-charged (i.e., +2 and +3) peaks with the four most abundant ions were selected for collision-induced dissociation. The MS/MS spectra were collected for each of these top four ions. The parent ion was excluded if the same parent ion was observed within 90 seconds. Collision energies were set to 10 V for the MS scan and 30 V for the MS/MS scan. Mass spectra were processed using MassLynx 4.0 (Waters) to export the .pkl files containing MS/MS peak lists. Protein identification was performed using .pkl files on the online MASCOT Server (http://www.matrixscience.com). The settings of the MASCOT parameters were (1) digesting enzyme, trypsin; (2) missed cleavage site, one; (3) variable modification, carbamidomethylation (cysteine) and oxidation (methionine, histidine, and tryptophan); (4) peptide tolerance, <300 ppm; and (5) mass values, MH^+ and monoisotopic. Only proteins with Molecular Weight Search scores above the significance levels were considered to be positively identified.

2.5. *Functional classification*

Sequences of all identified proteins by MS were submitted to KOGnitor (http://www.ncbi.nlm.nih.gov/COG/grace/kognitor.html) for eukaryotic orthologous group (KOG) classification by a customized Perl script. Nearly all identified proteins can be assigned a KOG number. A KOG number usually belongs to one category, although some KOG numbers may belong to more than one category. Thus, when counting the number of total proteins with functional classifications, the proteins associated with more than one category were counted more than once. The protein ratio for each category was calculated by dividing the number of proteins within a category by the sum of assigned proteins from all categories.

3. Results

3.1. *High-fructose diet-induced MetS in a rat model*

To assess the efficacy of high-fructose consumption to induce MetS in the rat model, we analyzed indicators of MetS such as body weight, blood pressure, and several blood biochemistry parameters. As shown in Table 1, after consuming a 60% high-fructose diet supplement for 16 weeks, the SD rats had significantly higher blood pressure, higher concentrations of glucose, insulin, triglycerides, and cholesterol, compared with the rats maintained on the control chow diet.

Table 1 – Body weight and biochemical parameters in the control group versus the metabolic syndrome group.

Group	Control	MetS (high-fructose diet)
Body weight (g)	540.8 ± 70.6	560.2 ± 100.1
Glucose (mg/dL)	116.0 ± 3.6	127.5 ± 5.0*
Insulin (ng/mL)	0.3 ± 0.13	0.8 ± 0.29*
Triglyceride (mg/dL)	78.1 ± 15.3	271.3 ± 124.9*
Cholesterol (mg/dL)	66.1 ± 11.6	107.6 ± 25.7*
Blood pressure (mmHg)	104.1 ± 3.0	129.2 ± 8.2*
TBARS (nmol MDA/mg protein)	0.04 ± 0.01	0.08 ± 0.01*

The values are presented as the mean ± the standard deviation ($n = 8$).
*Indicates $p < 0.05$, compared with the control group. Statistical analysis is based on the two sample t test.
MDA = malondialdehyde; MetS = metabolic syndrome; TBARS = thiobarbituric acid-reactive substances.

3.2. *Comparison of liver proteome between the control and the high-fructose-fed rats*

To gain insight into the molecular mechanism underlying MetS in the high-fructose-fed rat model, we employed a 2-D gel electrophoresis-based proteomics assessment to evaluate the differential protein expression profiles of the liver tissue. The liver was studied because it is the major metabolic organ that responds to MetS induction in rats. As shown in Figures 1 and 2, total liver protein extracts were obtained separately from the control and MetS rats, and 2-D gel electrophoresis was used to display the hepatic protein expression patterns and identify differences. After comparing the density of green and red fluorescence, which indicates every individual protein expressed in the liver tissue of the control and MetS rats, respectively, 21 spots were examined. Of these, using the merged fluorescent color, 10 spots were identified as having a significant change of expression ($p < 0.05$) that was larger than 1.5-fold. The proteins with a merged yellow color indicated no

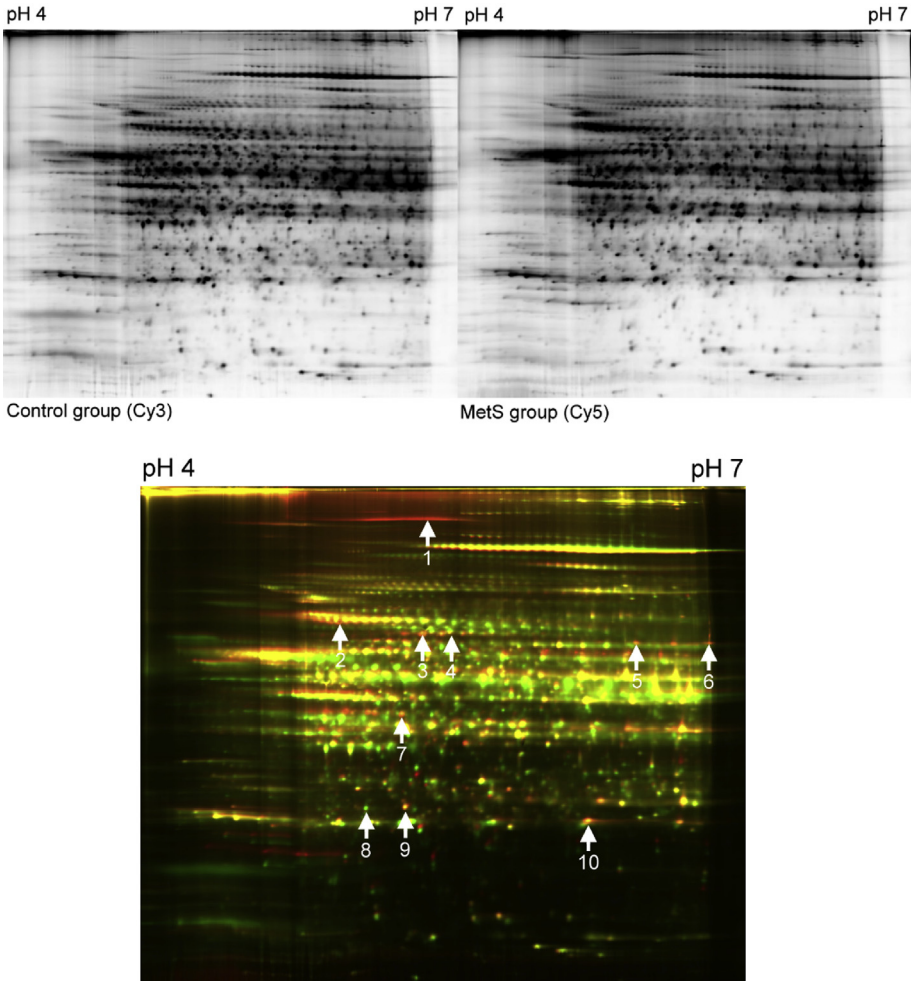

Figure 1 – Two-dimensional difference gel electrophoresis (2D-DIGE) analysis of the rat liver in the metabolic syndrome (MetS) group (Cy 5) versus the control group (Cy3). Analysis of the resulting 2D-DIGE gel images show 10 protein spots are differentially expressed between the MetS and control groups. Of these, eight protein spots are upregulated and two protein spots are downregulated. Differentially expressed protein spots were excised from preparative gels, in-gel digested with trypsin, and analyzed using MALDI-TOF/MS-MS. Several proteins are represented by spots. MALDI-TOF/MS-MS = Matrix-assisted laser desorption/ionization-time-of-flight/mass spectroscopy-mass spectroscopy.

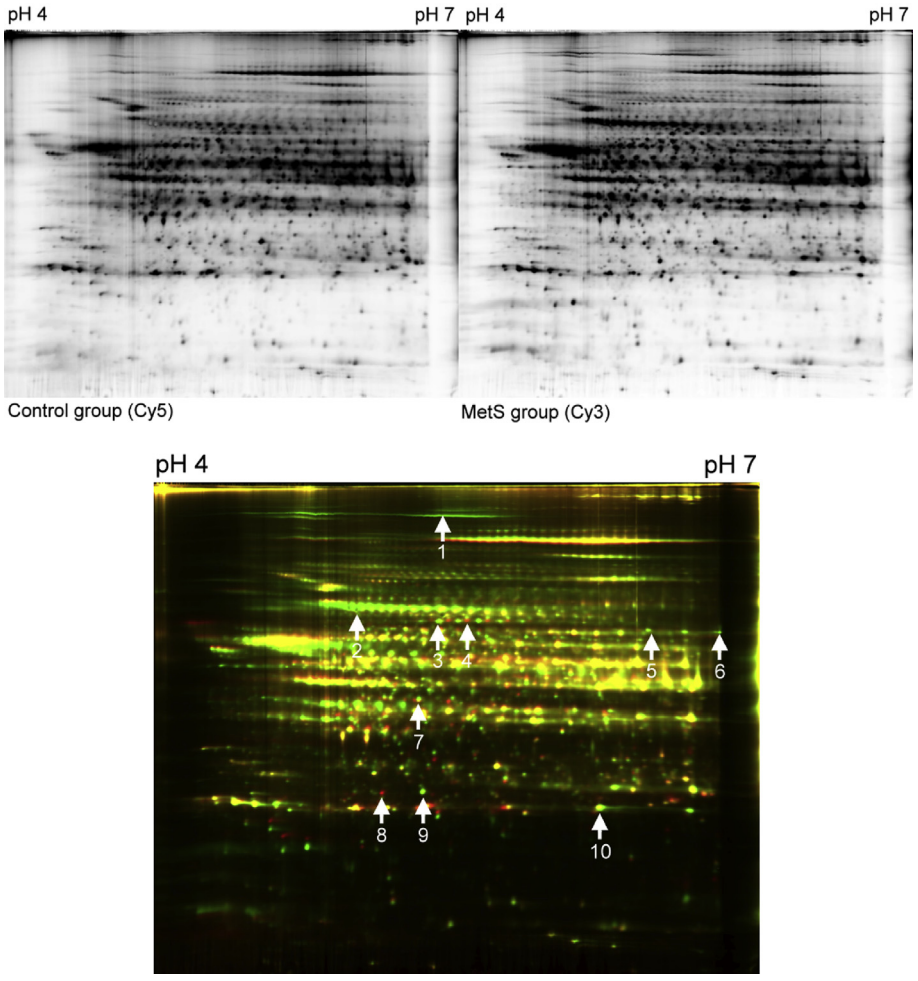

Figure 2 – Two-dimensional difference gel electrophoresis (2D-DIGE) analysis of the rat liver in MetS group (Cy 3) versus control group (Cy5). Analysis of the resulting 2D-DIGE gel images showed 10 protein spots are differentially expressed between the MetS and control groups. Of these, eight protein spots are upregulated and two protein spots are downregulated. Differentially expressed protein spots were excised from preparative gels, in-gel digested with trypsin, and analyzed using MALDI-TOF/MS-MS. Several proteins are represented by spots. MALDI-TOF/MS-MS, matrix-assisted laser desorption/ionization-time-of-flight/mass spectroscopy-mass spectroscopy.

difference in expression between the control and high-fructose-fed groups. Green indicated higher protein expression in the control group, and red indicated higher protein expression in the MetS groups. Green and red protein spots were removed from the gels and subjected to ESI-MS/MS proteomics. As summarized in Table 2, these differentially expressed proteins, which may be responsive to the pathogenesis of MetS, fall into five categories, based on their functional properties, which includes (1) carbohydrate metabolism/synthesis: fructose-1,6-bisphosphatase 1 (FBPase) and the pyruvate dehydrogenase complex component E2 (PDC-E2); (2) fatty acid metabolism/synthesis: fatty acid synthase (FAS) and acyl-coenzyme A synthetase 1 (ACSM1); (3) antioxidants: glutathione S-transferase alpha 3, peroxiredoxin I; (4) molecular chaperone: 78 kDa glucose-regulated protein (GRP78); and (5) others: bifunctional ATP-dependent dihydroxyacetone kinase/FAD-AMP lyase (riboflavin-cyclic-4′,5′-phosphate-forming), glial fibrillary acidic protein (GFAP), and Rho GDP-dissociation inhibitor 1 (RhoGDI1). Among the proteins, ASCM1 and Rho GDP-dissociation inhibitor 1 are downregulated by the high-fructose diet, and the other eight proteins are upregulated.

4. Discussion

Metabolic syndrome encompasses carbohydrate and lipid metabolism disorders. The present study used a rat model fed a high-fructose diet that reflected the clinical parameters present in human MetS patients such as abnormal lipid concentration in plasma coupled with high blood pressure and insulin resistance. Our liver proteome analysis revealed that enzymes involved in gluconeogenesis such as FBPase, a regulatory enzyme in gluconeogenesis that is elevated by obesity and dietary fat intake, is induced by the high-fructose diet. Fructose-1,6-bisphosphatase 1 is an important gluconeogenic enzyme that catalyzes the hydrolysis of fructose 1,6-bisphosphate to fructose 6-phosphate and phosphate [14]. A potential basis for

Table 2 – The differential expression of liver proteins in rat in the theme group versus the control group.

No.	Protein name	Protein ID	MW (Da)	Function	Regulation
1	Fatty acid synthase	P12785	272,650	Fatty acid biosynthetic process	Up
2	78 kDa glucose-regulated protein	P06761	72,347	Unfolded protein binding	Up
3	Dihydrolipoyllysine-residue Acetyltransferase component of pyruvate dehydrogenase complex, mitochondrial	P08461	67,166	Acetyl-CoA biosynthetic process from pyruvate, glycolysis	Up
4	Acyl-coenzyme A synthetase, mitochondrial	Q91VA0	64,760	Fatty acid metabolism	Down
5	Bifunctional ATP-dependent dihydroxyacetone kinase/FAD-AMP lyase (riboflavin-cyclic-4′,5′-phosphate-forming)	Q4KLZ6	59,444	Glycerol metabolic process	Up
6	Glial fibrillary acidic protein	P47819	49,957	Cell-specific marker	Up
7	Fructose-1,6-bisphosphatase 1	P19112	39,609	Cellular response to insulin stimulus, fructose 6-phosphate metabolic process, gluconeogenesis	Up
8	Rho GDP-dissociation inhibitor 1	Q5XI73	23,407	GTPase activator activity	Down
9	Glutathione S-transferase alpha 3	B0BNI1	23,961	Aromatic amino acid family metabolic process, transferase activity	Up
10	Peroxiredoxin I	Q63716	22,109	Cell redox homeostasis, oxidation reduction, response to oxidative stress	Up

ATP = adenosine triphosphate; MW = molecular weight.

the augmented hepatic expression of FBPase is to accommodate increased fructose catabolism and favor energy storage in high-fructose-fed rats. In addition, PDC-E2, an enzyme component of the multienzyme pyruvate dehydrogenase complex, was elevated in our MetS induced rats. The pyruvate dehydrogenase complex is responsible for pyruvate decarboxylation to produce acetyl-CoA, which is the basic building block of fatty acids. It is reasonable that after high-fructose consumption, the extra energy influx increases both gluconeogenesis (we observed the upregulation of FBPase) and lipid synthesis. In accordance with this idea, the key enzymes for lipid synthesis such as fatty acid synthase (FAS) were elevated in MetS rats Fatty acid synthase may have a role in regulating body weight and in the development of obesity [15,16]. Expression of the FAS gene and FAS activity are increased by insulin in cultured human adipocytes, which suggests that insulin may modulate their function [17]. Moreover, higher levels of FAS mRNA and protein were observed in insulin-resistant large adipocytes, compared with small adipocytes in wild-type mice [18,19], which is consistent with our finding that insulin resistance is coupled with increased FAS protein. Recent studies have reported that inhibition of FAS in rodents induces profound weight loss and reduced food intake, suggesting that FAS may be involved in obesity through regulation of feeding behavior and energy homeostasis [15,20]. In our rat model, the high-fructose diet significantly increased abdominal fat pad weight and serum triacylglycerol concentration (78.1 ± 15.3 mg/dL in the control rats, 271.3 ± 124.9 mg/dL in high-fructose-fed rats). It is possible that increased FAS expression enhances the synthesis of fatty acids and the consequent deposition of lipid in adipose tissue, along with fatty acid release into the circulation, as observed in the MetS rats. We also observed reduced ACSM1 expression in rats fed a high-fructose diet. Acyl-coenzyme A synthetase 1 belongs to a large family of enzymes that catalyze the activation of fatty acids by coenzyme A to produce acyl-CoA, the first step in fatty acid metabolism. As previously reported, mice lacking ACSL1 specifically in adipose tissue have defects in adipose fatty acid oxidation [21]. It is possible that high-fructose consumption leads to excess fatty acid synthesis by FAS and reduces fatty acid metabolism by ACSM1, thus causing hyperlipidemia in the rat model.

Glucose-regulated protein was discovered as a cellular protein induced by glucose starvation [22]. It is a member of the HSP70 protein family that is primarily present in the endoplasmic reticulum (ER). It functions as a major chaperone that is involved in many cellular processes such as protein folding and assembly, marking misfolded proteins for proteosomal degradation [23], regulating calcium (Ca^{2+}) homeostasis, and serving as a sensor for ER stress [24]. Excessive fat storage stimulates ER stress in liver and adipose tissue, which subsequently activates inositol-requiring enzyme 1 (IRE-1) and the downstream kinase, c-Jun NH2 -terminal kinase (JNK), through the ER stress signaling pathway. Active JNK can phosphorylate the insulin receptor substrate (IRS)-1 on Ser307, thus inhibiting tyrosine phosphorylation of IRS-1 and the downstream insulin signaling pathway, thereby resulting in insulin resistance [25]. Our result showed increased GRP78 in the MetS rat, which correlates with insulin resistance, was consistent with the findings of other research groups.

In this study, we have identified two antioxidant proteins, glutathione S-transferase and peroxiredoxins, that were upregulated with the high-fructose diet. Some reports have mentioned the effects of antioxidants as being protective against oxidative stress. Evidence is fast growing that oxidative stress is important not only for normal cell physiology but also for many pathological processes such as atherosclerosis, neurodegenerative diseases, and cancer [26–28]. Reactive oxygen species (ROS) participate in carcinogenesis at all stages such as initiation, promotion, and progression. Nevertheless,

studies of the expression and activity of glutathione S-transferases during diabetes are inconclusive. Both increased and decreased hepatic expression of glutathione S-transferases have been reported *in vitro* and *in vivo*. A similar situation exists for peroxiredoxins, a family of antioxidative proteins. Peroxiredoxins are capable of protecting cells from ROS toxicity and regulating signal transduction pathways that influence cell growth and apoptosis [26]. *In vitro*, the peroxiredoxin genes I–IV are overexpressed when hydrogen peroxide (H_2O_2) concentrations in cells are elevated [29]. Bast et al [30] reported that expression of peroxiredoxin I is up-regulated in cultured insulinoma cells exposed to various stress agents such as diabetogenic compounds such as alloxan and streptozotocin. Consistent with these data, we have seen that the high-fructose diet-fed rats exhibited a higher expression of antioxidant proteins. It is reasonable that development of MetS may be coupled with ROS production, which in turn induces the antioxidant proteins.

Glial fibrillary acidic protein is an intermediate filament protein that is expressed by numerous cell types of the central nervous system such as astrocytes and ependymal cells. Glial fibrillary acidic protein immunoreactivity was detected in rat and in human hepatic stellate cells (HSCs), which exhibit neural/neuroendocrine features. In the rat liver, GFAP increases in the acute response to injury and decreases in the chronic response [31]. The activation of HSCs involves the conversion of quiescent cells into proliferative, contractile, and fibrogenic myofibroblasts. Glial fibrillary acidic protein expression in the liver is an early marker of stellate cell activation [32]. Liver inflammation is the hallmark of early-stage liver fibrosis, and ultimately results in HSC activation and extracellular matrix deposition [33]. We did not study tissue histology; however, it is possible that hyperlipidemia induced by high-fructose diet enhances lipid deposition in the liver, and activates the inflammation signal transduction pathways that activate stellate cells and induces the expression of GFAP.

Rho GDP-dissociation inhibitor, an intracellular signaling effector, is responsive to sequester Rho GTPases in their inactive GDP-bound states. Rho GTPases have been implicated in diverse cellular functions and are potential therapeutic targets in inflammation, cancer, and neurologic diseases [34,35]. It is possible that a high-fructose diet may down-regulate the expression of RhoGDI1, and thus activate Rho, which may contribute to the inflammation state in MetS rats.

Bifunctional ATP-dependent dihydroxyacetone kinase/FAD-AMP lyase was first discovered in rat liver extracts [36], and is the only known enzymatic source of the unusual flavin nucleotide riboflavin 4′,5′-cyclic phosphate (FMN). Inducible nitric oxide synthase (iNOS), which is an inflammation marker, has reduced activity on the loss of the FMN binding ability. It is possible that high-fructose diet-induced FAD-AMP lyase provides FMN to facilitate the inflammation-enhancing function of iNOS. However, the physiological influence of FAD-AMP lyase on MetS still needs to be further confirmed.

5. Conclusions

In summary, our results provide molecular mechanisms that underlie the abnormal blood biochemistry of MetS. We also identified many new targets within the liver for future investigation (Figure 3). Our results show that ER stress, inflammation, and oxidation-related proteins are expressed coincidently with the onset of insulin resistance and may be implicated directly in hepatic complications of insulin resistance, insulin signaling attenuation, and/or lipoprotein dysregulation. Further characterization of these proteins and their potential involvement in the link between insulin resistance and metabolic dyslipidemia is needed.

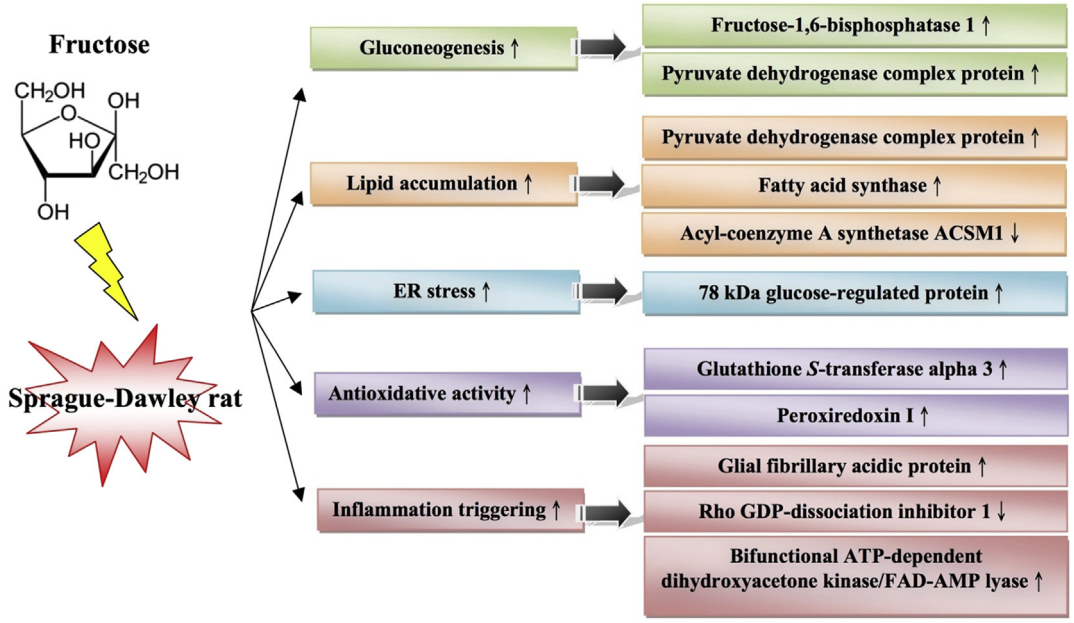

Figure 3 – Proposed signaling transduction pathway, which is interfered by high fructose induction. ER = endoplasmic reticulum. The up arrows indicate upregulation and the down arrows indicate downregulation.

Conflicts of interest

All contributing authors have no conflicts of interest to declare.

Acknowledgments

This work was financially supported by Grants NSC 98-2313-B002-064 from the National Science Council, Taipei City, Taiwan, Republic of China.

REFERENCES

[1] Alberti KG, Zimmet P, Shaw J. Metabolic syndrome—a new world-wide definition. A consensus statement from the International Diabetes Federation. Diabet Med 2006;23:469–80.
[2] Minehira K, Tappy L. Dietary and lifestyle interventions in the management of the metabolic syndrome: present status and future perspective. Eur J Clin Nutr 2002;56:7.
[3] Aude YW, Mego P, Mehta JL. Metabolic syndrome: dietary interventions. Curr Opin Cardiol 2004;19:473–9.
[4] Fonseca VA. The metabolic syndrome, hyperlipidemia, and insulin resistance. Clin Cornerstone 2005;7(2–3):61–72.
[5] Chen CL, Pan TM. Effects of red mold dioscorea with pioglitazone, a potentially functional food, in the treatment of diabetes. J Food Drug Anal 2015;23:719–28.
[6] Grundy SM. Does a diagnosis of metabolic syndrome have value in clinical practice? Am J Clin Nutr 2006;83:1248–51.
[7] Bray GA, Nielsen SJ, Popkin BM. Consumption of high-fructose corn syrup in beverages may play a role in the epidemic of obesity. Am J Clin Nutr 2004;79:537–43.
[8] Rutledge AC, Adeli K. Fructose and the metabolic syndrome: pathophysiology and molecular mechanisms. Nutr Rev 2007;65(6 Pt 2):S13–23.
[9] Hwang IS, Ho H, Hoffman BB, Reaven GM. Fructose-induced insulin resistance and hypertension in rats. Hypertension 1987;10:512–6.
[10] Barros CM, Lessa RQ, Grechi MP, Mouco TL, Souza MG, Wiernsperger N, Bouskela E. Substitution of drinking water by fructose solution induces hyperinsulinemia and hyperglycemia in hamsters. Clinics (Sao Paulo) 2007;62:327–34.
[11] Taghibiglou C, Carpentier A, Van Iderstine SC, Chen B, Rudy D, Aiton A, Lewis GF, Adeli K. Mechanisms of hepatic very low density lipoprotein overproduction in insulin resistance. Evidence for enhanced lipoprotein assembly, reduced intracellular ApoB degradation, and increased microsomal triglyceride transfer protein in a fructose-fed hamster model. J Biol Chem 2000;275:8416–25.
[12] Le KA, Tappy L. Metabolic effects of fructose. Curr Opin Clin Nutr Metab Care 2006;9:469–75.
[13] Chen KN, Peng WH, Hou CW, Chen CY, Chen HH, Kuo CH, Korivi M. *Codonopsis javanica* root extracts attenuate hyperinsulinemia and lipid peroxidation in fructose-fed insulin resistant rats. J Food Drug Anal 2013;21:347–55.
[14] Lamont BJ, Visinoni S, Fam BC, Kebede M, Weinrich B, Papapostolou S, Massinet H, Proietto J, Favaloro J, Andrikopoulos S. Expression of human fructose-1,6-bisphosphatase in the liver of transgenic mice results in increased glycerol gluconeogenesis. Endocrinology 2006;147:2764–72.
[15] Loftus TM, Jaworsky DE, Frehywot GL, Townsend CA, Ronnett GV, Lane MD, Kuhajda FP. Reduced food intake and body weight in mice treated with fatty acid synthase inhibitors. Science 2000;288:2379–81.
[16] Kovacs P, Harper I, Hanson RL, Infante AM, Bogardus C, Tataranni PA, Baier LJ. A novel missense substitution (Val1483Ile) in the fatty acid synthase gene (FAS) is associated with percentage of body fat and substrate oxidation rates in nondiabetic Pima Indians. Diabetes 2004;53:1915–9.
[17] Claycombe KJ, Jones BH, Standridge MK, Guo Y, Chun JT, Taylor JW, Moustaid-Moussa N. Insulin increases fatty acid synthase gene transcription in human adipocytes. Am J Physiol 1998;274(5 Pt 2):R1253–9.
[18] Bluher M, Michael MD, Peroni OD, Ueki K, Carter N, Kahn BB, Kahn CR. Adipose tissue selective insulin receptor knockout protects against obesity and obesity-related glucose intolerance. Dev Cell 2002;3:25–38.
[19] Bluher M, Patti ME, Gesta S, Kahn BB, Kahn CR. Intrinsic heterogeneity in adipose tissue of fat-specific insulin receptor knock-out mice is associated with differences in patterns of gene expression. J Biol Chem 2004;279:31891–901.
[20] Kumar MV, Shimokawa T, Nagy TR, Lane MD. Differential effects of a centrally acting fatty acid synthase inhibitor in lean and obese mice. Proc Natl Acad Sci USA 2002;99:1921–5.
[21] Ellis JM, Li LO, Wu PC, Koves TR, Ilkayeva O, Stevens RD, Watkins SM, Muoio DM, Coleman RA. Adipose acyl-CoA synthetase-1 directs fatty acids toward beta-oxidation and is required for cold thermogenesis. Cell Metab 2010;12:53–64.
[22] Lee AS. GRP78 induction in cancer: therapeutic and prognostic implications. Cancer Res 2007;67:3496–9.
[23] Ni M, Lee AS. ER chaperones in mammalian development and human diseases. FEBS Lett 2007;581:3641–51.
[24] Li J, Lee AS. Stress induction of GRP78/BiP and its role in cancer. Curr Mol Med 2006;6:45–54.
[25] Hirosumi J, Tuncman G, Chang L, Gorgun CZ, Uysal KT, Maeda K, Karin M, Hotamisligil GS. A central role for JNK in obesity and insulin resistance. Nature 2002;420:333–6.
[26] Klaunig JE, Xu Y, Isenberg JS, Bachowski S, Kolaja KL, Jiang J, Stevenson DE, Walborg Jr EF. The role of oxidative stress in chemical carcinogenesis. Environ Health Perspect 1998;106(Suppl. 1):289–95.
[27] Dhalla NS, Temsah RM, Netticadan T. Role of oxidative stress in cardiovascular diseases. J Hypertens 2000;18:655–73.
[28] Ambrosone CB. Oxidants and antioxidants in breast cancer. Antioxid Redox 2000;2:903–17.
[29] Mitsumoto A, Takanezawa Y, Okawa K, Iwamatsu A, Nakagawa Y. Variants of peroxiredoxins expression in response to hydroperoxide stress. Free Radic Biol Med 2001;30:625–35.
[30] Bast A, Wolf G, Oberbaumer I, Walther R. Oxidative and nitrosative stress induces peroxiredoxins in pancreatic beta cells. Diabetologia 2002;45:867–76.
[31] Niki T, De Bleser PJ, Xu G, Van Den Berg K, Wisse E, Geerts A. Comparison of glial fibrillary acidic protein and desmin staining in normal and CCl4-induced fibrotic rat livers. Hepatology 1996;23:1538–45.
[32] Morini S, Carotti S, Carpino G, Franchitto A, Corradini SG, Merli M, Gaudio E. GFAP expression in the liver as an early marker of stellate cells activation. Ital J Anat Embryol 2005;110:193–207.
[33] Seki E, De Minicis S, Gwak GY, Kluwe J, Inokuchi S, Bursill CA, Llovet JM, Brenner DA, Schwabe RF. CCR1 and CCR5 promote hepatic fibrosis in mice. J Clin Invest 2009;119:1858–70.
[34] Sahai E, Marshall CJ. RHO-GTPases and cancer. Nat Rev Cancer 2002;2:133–42.
[35] Boettner B, Van Aelst L. The role of Rho GTPases in disease development. Gene 2002;286:155–74.
[36] Fraiz FJ, Pinto RM, Costas MJ, Aavalos M, Canales J, Cabezas A, Cameselle JC. Enzymic formation of riboflavin 4′,5′-cyclic phosphate from FAD: evidence for a specific low-Km FMN cyclase in rat liver1. Biochem J 1998;330(Pt 2):881–8.